Solution Equilibrium Studies of Anticancer Ruthenium(II)-η^6-*p*-cymene Complexes of Pyridinecarboxylic Acids

Éva Sija[a,b], Christian G. Hartinger[c,d], Bernhard K. Keppler[d], Tamás Kiss[a,b], Éva A. Enyedy[a,*]

[a] *Department of Inorganic and Analytical Chemistry, University of Szeged, 6720 Szeged, Hungary*

[b] *HAS-USZ Bioinorganic Chemistry Research Group, 6720 Szeged, Hungary*

[c] *The University of Auckland, School of Chemical Sciences, 1142 Auckland, New Zealand*

[d] *Institute of Inorganic Chemistry, University of Vienna, 1090 Vienna, Austria*

Keywords: Speciation, Stability constants, Antitumor agents, Picolinic acid, Dipicolinic acid

ABSTRACT

Stoichiometry and stability of antitumor ruthenium(II)-η^6-*p*-cymene complexes of picolinic acid and its 6-methyl and 6-carboxylic acid derivatives were determined by pH-potentiometry, ^{1}H NMR spectroscopy and UV/Vis spectrophotometry in aqueous solution in the presence or absence of coordinating chloride ions. The picolinates form exclusively mono-ligand complexes in which they can coordinate via the bidentate (O,N) mode and a chloride or a water molecule is found at the third binding site of the ruthenium(II)-η^6-*p*-cymene moiety depending on the conditions. [Ru(η^6-*p*-cymene)(L)(H_2O/Cl)] species are predominant at physiological pH in all studied cases. Hydrolysis of the aqua complex or the chlorido/hydroxido co-ligand exchange results in the formation of the mixed-hydroxido species [Ru(η^6-*p*-cymene)(L)(OH)] in the basic pH range. There is no indication for the decomposition of the mono-ligand complexes during 24 h in the ruthenium(II)-η^6-*p*-cymene−picolinic acid system between pH 3 and 11; however, a slight dissociation with a low reaction rate was found in the other two systems leading to the appearance of the dinuclear trihydroxido-bridged species $[Ru_2(\eta^6\text{-}p\text{-cymene})_2(OH)_3]^+$ and free ligands at pH > 10. The replacement of the chlorido by an aqua ligand in [Ru(η^6-*p*-cymene)(L)Cl] was also monitored and equilibrium constants for the exchange process were determined.

* Corresponding author. Tel.: +36 62 544334; fax: +36 62 420505.

E-mail address: enyedy@chem.u-szeged.hu (É. A. Enyedy).

1. Introduction

More and more people are diagnosed with cancer and one out of four in Europe and the US die of cancer [1,2]. The clinical success of cis-diamminedichloridoplatinum(II), cisplatin, has opened new avenues in cancer treatment. Although platinum-based drugs (and other chemotherapeutics) have undoubtedly many beneficial properties, treatment is paralleled by serious adverse effects and the development of resistance phenomena, which are limiting factors for curative treatment [3-5]. For this reason there is an on-going demand for the development of novel antitumor agents. In order to reduce the toxic effects of metal-based anticancer agents, Pt(IV) and other metal ions, such as Au(III), Ti(IV), Ga(III), Cu(II), Rh(III), Ru(III/II), were used in the design of new drug molecules. Some representatives have already entered and finished early clinical trial phases. These include titanocene dichloride [6] and [*tris*(8-quinolinolato)gallium(III)] [7]. However, most promising metal-based anticancer drug candidates in clinical trials are the Ru(III) containing imidazolium *trans*-[tetrachlorido(1H-imidazole)(dimethylsulfoxide-κ*S*)ruthenate(III)] (NAMI-A) and the *trans*-[tetrachloridobis(1H-indazole)ruthenate(III)] complexes KP1019 [8-10] and KP1339 [11]. KP1019 is efficient in colorectal carcinoma models, while NAMI-A is an antimetastatic agent which can affect the motility of the cancer cells [12,13]. The mode of action and the intracellular targets of Ru(III) complexes are not exactly known. There are many investigations suggesting that the intravenously injected drugs can be transported mainly by the serum albumin and/or transferrin in the blood plasma [14-18]. Reduction of Ru(III) compounds in the cytosol leads to the kinetically more labile and more reactive Ru(II) compounds. This is a result of the reductive atmosphere in tumours due to fast anabolic processes [9,19]. DNA and cellular proteins like kinases or other enzymes were suggested as intracellular targets [20,21].

More recently, organometallic pseudo octahedral "piano-stool" Ru(II)(η^6-arene) complexes with the metal ion stabilized in +2 oxidation state by different arene-type ligands have shown potential for the development of anticancer agents with a wide variety of modes of action [21-23]. They exhibit a well-balanced lipophilic/hydrophilic character to the complex allowing potential intravenous administration [22]. Such Ru(II) complexes feature in addition to the η^6-coordinated arene ligand, often a *p*-cymene, three available coordination sites. Ru(II)(η^6-*p*-cymene) complexes are usually prepared from reaction of the chlorido-bridged dinuclear complex [Ru(II)(η^6-*p*-cymene)Cl_2]$_2$ with mono- or bidentate ligands. In

aqueous solution the dimeric chlorido-bridged complex dissociates to monomeric species and hydrolyzes. The chlorido ligands can be exchanged partly or completely by aqua or hydroxido, depending on the chloride concentration and pH value [22-25]. These hydrolysis products are not anticancer active [26]. By careful selection of the ligands occupying the three other coordination sites the kinetics and pharmacological properties of these Ru(II) complexes can be modulated [27]. Ru(II)(η^6-*p*-cymene) complexes formed with bidentate (O,O) donor ligands such as the hydroxypyrones maltol and ethyl maltol show stronger cytotoxic effects than the dimeric Ru(II)(η^6-*p*-cymene) derivatives [28]. Cytotoxicity can be further improved by using ligands with (O,N), (N,N) or (O,S) donor systems. These comprise picolinic acid, thiomaltol, thioallomaltol, *etc.* [26,29-35]. The type of chelating ligands does not only have an influence on the biological properties but also impacts the stability of the complex formed by preventing hydrolysis of the Ru(II)(η^6-*p*-cymene) organometallic fragment. Furthermore, the ligand can also modify the interaction with different biomolecules such as albumin, transferrin or various cellular proteins. Grgurić-Šipka, Gligorijević and co-workers studied the biological activity of Ru(II)(η^6-*p*-cymene) complexes of various pyridine derivatives and moderate-to-low cytotoxicity was found in six tumour cell lines; although the complex of picolinic acid (pic) represents an enhanced antiproliferative activity [26,36]. As these complexes are considered as prodrugs, the knowledge of their speciation and the most plausible chemical forms in aqueous solution in the biologically relevant pH range is a mandatory prerequisite for understanding the alterations in their biological activity.

In the present work, solution equilibria of Ru(II)(η^6-p-cymene) fragments with pic, 6-methylpicolinic acid (6-Mepic) and pyridine-2,6-dicarboxylic acid (dipic) were studied (Chart 1) by the combination of various methods such as pH-potentiometry, UV/Vis and ^{1}H NMR spectroscopy in order to determine the composition and stability of complexes formed in aqueous solution. These stability data are compared with those of structurally related hydroxy(thio)pyrone complexes featuring bidentate (O,O) or (O,S) coordination modes investigated in earlier studies [37].

Chart 1

2. Experimental

2.1. Chemicals

Pic, 6-Mepic, dipic, KCl, KNO_3, $AgNO_3$, HCl, HNO_3 and KOH were purchased from Sigma-Aldrich and used without further purification. The purity of the ligands was checked and the exact concentrations of the ligand stock solutions were determined by pH-potentiometric titrations with the help of the computer program HYPERQUAD [38]. [Ru(II)(η^6-*p*-cymene)Cl_2]$_2$ was synthesized and purified according to a literature procedure [39]. A stock solution of [Ru(II)(η^6-*p*-cymene)(Z)$_3$] (where Z = H_2O and/or Cl^-; charges are omitted for simplicity) was obtained by dissolving a known amount of [Ru(II)(η^6-*p*-cymene)Cl_2]$_2$ in water; while the stock solution of [Ru(II)(η^6-*p*-cymene)$(H_2O)_3$]$(NO_3)_2$ was obtained from a solution of [Ru(II)(η^6-*p*-cymene)Cl_2]$_2$ in water after removal of chloride ions using equivalent amounts of $AgNO_3$. The exact concentration of the [Ru(II)(η^6-*p*-cymene)(Z)$_3$] stock solutions (with or without chloride) was determined with pH-potentiometric titrations employing literature data for [Ru(II)$_2$(η^6-*p*-cymene)$_2$(OH)$_i$] (i = 2 or 3) complexes [24,25].

2.2. pH-potentiometric measurements

The pH-potentiometric measurements for determination of the protonation constants of the ligands and the overall stability constants of the metal complexes were carried out at 25.0 ± 0.1 °C in water and at an ionic strength of 0.20 M KCl (for all the systems studied) or KNO_3 (in the case of pic) in order to keep the activity coefficients constant. The titrations were performed with carbonate-free KOH solution. The exact concentrations of HCl, HNO_3, KOH solutions were determined by pH-potentiometric titrations. An Orion 710A pH-meter equipped with a Metrohm combined electrode (type 6.0234.100) and a Metrohm 665 Dosimat burette were used for the pH-potentiometric measurements. The electrode system was calibrated to the pH = $-\log[H^+]$ scale by means of blank titrations (strong acid *vs.* strong base: HCl/HNO_3 *vs.* KOH), as suggested by Irving *et al.* [40]. The average water ionization constant, pK_w, was determined as 13.76 ± 0.01 at 25.0 °C, I = 0.20 M (KCl, KNO_3), which corresponds well to the literature [41]. The reproducibility of the titration points included in the calculations was within 0.005 pH. The pH-potentiometric titrations were performed in the pH range 2.0−11.5 and the maximum waiting time was ~15 min at each point. The initial volume of the samples was 10.0 mL. The ligand concentration was 2.0 mM and metal ion-to-ligand ratios of 1:1 to 1:3 were used. The accepted fitting of the titration curves was always less than 10 μL. Samples were degassed by bubbling purified argon through them for *ca.* 10 min prior to the measurements and it was also passed over the solutions during the titrations.

The computer program PSEQUAD [42] was utilized to establish the stoichiometry of the complexes and to calculate the overall stability constants. $\beta(M_pL_qH_r)$ is defined for the general equilibrium:

$$pM + qL + rH \rightleftharpoons M_pL_qH_r \quad \text{as } \beta(M_pL_qH_r) = [M_pL_qH_r]/[M]^p[L]^q[H]^r \qquad (1)$$

where M denotes the metal moiety [Ru(II)(η^6-*p*-cymene)Z_3] and L the completely deprotonated ligand, which is L^- for pic and 6-Mepic and L^{2-} for dipic. Literature logβ values of the various [$Ru_2(\eta^6$-*p*-cymene$)_2(OH)_i$] complexes were used in the absence and presence of chloride ions [24,25] and compared to data collected in the course of the experiments described herein. In all calculations exclusively titration data were used from experiments in which no precipitate was visible in the reaction mixture.

2.3. UV/Vis spectrophotometric and ^{1}H NMR measurements

A Hewlett Packard 8452A diode array spectrophotometer was used to record the UV/Vis spectra in the interval 200–800 nm. The path length was 1 cm. Protonation and stability constants and the individual spectra of the species were calculated with the computer program PSEQUAD [42]. The spectrophotometric titrations were performed on samples of the ligands alone or with [Ru(II)(η^6-*p*-cymene)$(Z)_3$] over the pH range 2.0–11.5 at an ionic strength of 0.20 M (KCl or KNO_3) and at 25.0 ± 0.2 °C. The concentration of ligands was set constant at 0.12 mM or 0.32 mM in chloride free system and the metal-to-ligand ratios were 1:1 and 1:2. UV/Vis measurements for [Ru(II)(η^6-*p*-cymene)$(Z)_3$]−pic systems were carried out at 1:1 metal-to-ligand ratio by preparing individual samples in which KCl or KNO_3 was partially or completely replaced by HCl or HNO_3 and pH values, varying in the range *ca.* 0.8–2.0, were calculated from the HCl or HNO_3 content.

^{1}H NMR studies were carried out on a Bruker Ultrashield 500 Plus instrument. 4,4-Dimethyl-4-silapentane-1-sulfonic acid was used as an internal NMR standard. The ligands were dissolved in a 10% (v/v) D_2O/H_2O mixture to yield a concentration of 1 mM and were titrated at 25 °C and I = 0.20 M (KCl, KNO_3) in absence or presence of [Ru(II)(η^6-*p*-cymene)$(Z)_3$] at 1:1 and 1:2 metal-to-ligand ratios. During the ^{1}H NMR titrations the maximum waiting time was ~30 min at each point, however in case of some samples spectra were recorded after 24 h as well. Samples contained [Ru(II)(η^6-*p*-cymene)$(Z)_3$] and the pic ligand at various ratios (1:1−1:4) at constant concentration of the ligand (2×10^{-3} M) at pH 3.2. The ^{1}H NMR spectra were recorded to study the H_2O/Cl^- exchange processes in the [Ru(II)(η^6-*p*-cymene)(L)*Z*] complexes at pH 3.2 (pic and dipic) and at pH 4.3 (6-Mepic) in

dependence of the Cl^- concentration (0−500 mM). Protonation and stability constants were calculated with the computer program PSEQUAD [42].

3. Results and discussion

3.1. Proton dissociation processes of the ligands

The ligands chosen for these studies are derived from 2-picolinic acid (Chart 1). Their pK_a values as determined by pH-potentiometry and ^{1}H NMR spectroscopy are in reasonably good agreement with those reported in literature (Tables 1 and S1) [43-45].

Table 1

3.2. Complex equilibria of Ru(II)(η^6-p-cymene) with picolinic acid in chloride-free medium

The complex formation processes of pic with [Ru(II)(η^6-*p*-cymene)$(H_2O)_3$]$^{2+}$ were studied by pH-potentiometry, UV/Vis spectrophotometry and ^{1}H NMR spectroscopy in the presence of 0.2 M KNO_3. The hydrolytic equilibrium of the organometallic moiety establishes quickly in the absence of chloride ions in a quite simple manner. The stability constant of the dinuclear hydrolysis product [Ru(II)$_2$(η^6-*p*-cymene)$_2(OH)_3$]$^+$ was determined by pH-potentiometric and UV/Vis titrations of [Ru(II)(η^6-*p*-cymene)$(H_2O)_3$]$^{2+}$ and logβ (M_2H_{-3}) = −9.36(2) and −9.33(2) were calculated (see Table 1), respectively, which are in good agreement with data obtained by Buglyó *et al.* [25]. Analysis of the pH-potentiometric titration curves indicates that complex formation with pic is almost complete at the beginning of the titration at pH ~2. Therefore, the stability constant of [Ru(II)(η^6-*p*-cymene)(L)(H_2O)]$^+$ (denoted [ML]$^+$) was determined by pH-dependent UV/Vis measurements in the pH range of 0.8–2 (Table 1). Individual samples were prepared, in which KNO_3 was partially or completely replaced by HNO_3 keeping the ionic strength constant and the actual pH was calculated based on the strong acid content (Fig. S1). The logβ value of species [ML]$^+$ was kept constant during the calculation of the stability constant of complex [MLH_{-1}] from the pH-potentiometric data (Table 1). In addition, UV/Vis spectra were collected in the pH range 2–11 (Fig. S1) and the logβ value of species [MLH_{-1}] was also calculated from the spectral changes. The stability constants of species [MLH_{-1}] obtained by both methods are in good agreement with each other. Furthermore, these results were complemented by ^{1}H NMR titrations. Due to the slow ligand exchange processes with respect to the NMR time scale ($t_{1/2}$(obs) > ~1 ms), the

chemical shifts of the protons of the free and bound ligand and the [Ru(II)(η^6-*p*-cymene)] fragment are clearly distinguishable in the spectra (Fig. 1).

Fig. 1

^{1}H NMR spectra measured at 1:1 metal-to-ligand ratio at various pH values show the same picture about the speciation as the other two methods. Only one kind of complex, $[ML]^+$, predominates between pH 2.5 and 6.0 and there are no signals belonging to the non-bound ligand or to $[Ru(II)(\eta^6\text{-}p\text{-cymene})(H_2O)_3]^{2+}$. At pH > ~ 7 the hydrolysis of the complex $[ML]^+$ results in a gradually upfield shift of all peaks. The p*K* of the deprotonation of species $[ML]^+$ was estimated on basis of the pH-dependent shifts of the signals in the ^{1}H NMR spectra, and the value calculated (Table 1) is similar to that obtained by the pH-potentiometric and UV/Vis measurements. The distribution diagram calculated with the help of the logβ values of $[ML]^+$ and $[MLH_{-1}]$ shows that the decrease of the molar fraction of species $[ML]^+$ correlates well with the change of the chemical shifts of the *CH*(5) signal of the coordinated ligand due to the deprotonation (Fig. S2). It is noteworthy that the signals of the Ar(CH) protons of *p*-cymene moiety appear in four doublets instead of the two signals expected. Most probably Ru(II) can act as a chirality centre which results in the existence of two conformational isomers of the complexes in which the unsymmetrical bidentate ligand is coordinated [46,47], altough the intesity ratio of the doublets is changing by increasing pH as the ratio of the isomers is changing possibly.

In the complex $[ML]^+$ the bidentate (*O*,*N*) coordination mode of pic is the most probable in solution, as also suggested by a single-crystal X-ray diffraction study on the complex in the solid phase [48], and a water molecule probably occupies the last free site at the [Ru(II)(η^6-*p*-cymene)] fragment. The composition of $[MLH_{-1}]$ corresponds to a mixed hydroxido [ML(OH)] species formed by deprotonation of the coordinated water molecule of $[ML]^+$.

Partial decomposition of the complexes $[ML]^+$ and $[MLH_{-1}]$ formed in the [Ru(II)(η^6-*p*-cymene)]−pic system could be expected at high pH values, although the ^{1}H NMR spectra clearly show the absence of the trihydroxido dimeric complex $[M_2H_{-3}]^+$ and the uncoordinated ligand in the basic pH range even after 24 h (Figs. 1 and S3). The slow dissociation of the complex $[ML]^+$ was similar to that of hydroxypyridone complexes [49], for which however to a significant degree formation of the hydroxido-bridged dimer $[M_2H_{-3}]^+$ was detected. This was observed for Ru(II)(η^6-*p*-cymene) complexes of hydroxypyrones such as ethyl maltol [37] and maltol [49] at pH > 8.8 and already at pH 7.4, respectively in the mM concentration range in chloride-free medium.

3.3. Solution equilibria of Ru(II)(η^6-p-cymene) complexes of picolinic acid, 6-methyl picolinic acid and 2,6-dipicolinic acid in the presence of chloride ions

Chloride ions as competitive ligands are expected to affect the stabilities of Ru(II)(η^6-*p*-cymene)−pyridinecarboxylate complexes in aqueous solution, as it was also shown for hydroxypyrones [37]. The proton displacement from the ligands pic, 6-Mepic and dipic by the organometallic moiety is already significant at pH 2 (representative titration curves for dipic are shown in Fig. 2), but to a lesser extent compared with chloride-free medium. This is related to the ability of chloride ions to slightly suppress complexation. Thus, the logβ values determined in the presence of chloride ions are regarded as conditional stability constants and are valid only under the given conditions (0.2 M (KCl), T = 25.0 °C) owing to possible water/chlorido co-ligand exchange in the species [Ru(II)(η^6-*p*-cymene)Z_3] (denoted as M) and [Ru(II)(η^6-*p*-cymene)(L)Z] (denoted as [ML]; Z = H_2O or Cl^- and the charges of the complexes were omitted for simplicity).

Fig. 2

As the complex formation takes place already in the strongly acidic pH range in the three studied systems, the stability constants of species [ML] of pic, 6-Mepic and dipic (Table 1) were determined by deconvolution of the pH-dependent UV/Vis spectra (measured at pH 0.8–5.0). Spectra at pH < 2 were recorded for individual samples in which the KCl was partially or completely replaced by HCl and the actual pH values were calculated based on the HCl concentrations, while the changes of the metal-to-ligand charge-transfer (CT) and ligand bands were followed (see Fig. 3 for dipic). The direct comparison of the logβ [ML] of pic determined in the chloride-containing and in the chloride-free media (Table 1) clearly shows that the presence of chloride ions decreases the stability via the competition with the chelating ligand. A similar trend was observed for the analogous ethyl maltol complex [37]. Besides species [ML] of dipic formation of its protonated form [MLH] was also found in the strongly acidic pH range. The deprotonation of [MLH] takes place at pH < ~2.7, therefore, its pK(MLH) value could not be determined accurately by pH-potentiometric titrations. The stability constant of [MLH] could be fitted together with that of [ML] based on the recorded UV/Vis spectra (Fig. 3, Table 1), although with higher uncertainty since the whole deprotonation process could not be followed in the studied pH range. The deprotonation of [MLH] is accompanied by characteristic changes in the ^{1}H NMR spectra of the Ru(II)(η^6-*p*-cymene)–dipic system recorded at 1:1 metal-to-ligand ratio (Fig. 4), where neither free ligand nor Ru fragment is present even at pH 1.98. The significant upfield shift of the peaks

belonging to the aromatic protons of the ligand in the range 1.98 < pH < 2.74 strongly supports the formation of species [ML] from [MLH]. In the complex [MLH] most probably the ligand coordinates via its (N,O) donor set, while the non-coordinating carboxyl group is protonated. Dipic typically coordinates tridentately (*e.g.* in the complexes of Zn(II) [50], Cu(II) [51], $V(IV)O^{2+}$ [44], $V(V)O_2^+$ [44] or Ru(II) and Ru(III) [52]), however, binding through only two donor atoms (carboxylate-O and $N_{pyridine}$) in the [ML] complex of Ru(II)(η^6-*p*-cymene) is most likely. This ligand cannot act as a flexible tripodal binder which would be needed for the simultaneous coordination of the three donor atoms in a complex with "piano-stool" geometry.

Fig. 3

Fig. 4

Logβ values of the complexes [ML] (and [MLH] in the case of dipic) were kept constant during the evaluation of the pH-potentiometric data and UV/Vis spectra collected in the pH range of 2–11.5 and logβ values of the species $[MLH_{-1}]$ were determined (Table 1). These complexes, which are most probably mixed hydroxido species (*vide supra*), can be formed by the deprotonation of the coordinated water molecule or by the displacement of the chlorido ligand by the hydroxide at the third binding site of Ru(II)(η^6-*p*-cymene) moieties. The former process is accompanied by the upfield shift of the peaks of the aromatic protons of the coordinated ligand and *p*-cymene moiety at pH > 8 in the case of dipic (Fig. 4) and at pH > 7 in the case of pic (Fig. 5) and 6-Mepic (not shown). The pH-potentiometric titration curves indicate unambiguously hydrolytic processes in the pH range mentioned as it can be concluded from the base consumption exceeding the number of dissociable protons in the ligands (see Fig. 2 for dipic). However, the decomposition of [ML] (or $[MLH_{-1}]$) resulting in the trihydroxido dimeric complex $[M_2H_{-3}]^+$ would also contribute to the base consuming processes in the basic pH range.

Fig. 5

The ^{1}H NMR spectra of the Ru(II)(η^6-*p*-cymene)– pyridinecarboxylate systems recorded at 1:1 metal-to-ligand ratio in the basic pH range reveal that the [ML] complex of pic does not decompose up to pH 11, as peaks assignable neither to $[M_2H_{-3}]^+$ nor to the non-bound ligand were observed (Fig. 5). Decomposition of the Ru(II)(η^6-*p*-cymene) complexes of 6-Mepic (Fig. S4) and dipic (Fig. 4) is observed at a lesser extent at pH > ~10. This process is found to be relatively slow and could not be followed by pH-potentiometry accurately as the equilibria could not be reached during the time-scale of this method (max. ~15 min at each point). Therefore, the pH-potentiometric and UV/Vis data were evaluated only at pH < 10. It should

be noted that the hydroxido-bridged dimeric complex $[M_2H_{-3}]^+$ was not formed in the whole pH range studied when the ligand was added in excess, which can most probably protect the complex [ML] from the decomposition.

Comparison of the ^{1}H NMR spectra of the Ru(II)(η^6-*p*-cymene)–pic system recorded in the presence and absence of chloride ions (*cf.* Figs. 1 and 5) indicates that the spectra in KCl milieu are more complicated since additional peaks appear. All the peaks belonging to the complex [ML] appear in a double set with higher and lower intensities in the ^{1}H NMR spectra. Careful analysis of the spectra recorded at various chloride concentrations revealed that these signals belong to the aqua and to the chlorido complexes with compositions of [Ru(II)(η^6-*p*-cymene)(L)(H_2O)] and [Ru(II)(η^6-*p*-cymene)(L)(Cl)], respectively, which are in slow exchange processes with respect to the NMR time scale. It is noteworthy that these kinds of species were also formed but were not distinguishable in the case of the hydroxypyr(id)ones due to fast exchange processes [37,53]. The integrated areas of the corresponding peaks of complexes [Ru(II)(η^6-*p*-cymene)(L)(H_2O)] and [Ru(II)(η^6-*p*-cymene)(L)(Cl)] show at 0.2 M chloride concentration the presence of 7%, 15% and 51% aqua complex of pic, 6-Mepic and dipic, respectively (Figs. 4 and 5). The formation of the chlorido complexes of pic and 6-Mepic is more favourable compared with dipic and some hydroxypyr(id)ones [37,53].

The chlorido/aqua co-ligand exchange processes in [Ru(II)(η^6-*p*-cymene)(L)(Z)] of pic, 6-Mepic and dipic were investigated in detail by ^{1}H NMR spectroscopy. The spectral changes of $[Ru(II)(\eta^6\text{-}p\text{-cymene})(L)(H_2O)]^+$ were followed at various chloride concentrations at pH values at which the species [ML] predominate, *i.e.*, pH 3.2 for pic (Fig. 6) and dipic (Fig. S5) and 4.0 for 6-Mepic. Due to the well-separated ^{1}H NMR signals of the protons belonging to the aqua and chlorido complexes the integrated areas of the corresponding peaks could be calculated and converted to molar fractions. Based on the molar fractions log*K** values were obtained (Table 1) for the following equilibrium:

$$[Ru^{(II)}(\eta^6\text{-}p\text{-cymene})(L)(H_2O)] + Cl^- \rightleftharpoons [Ru^{(II)}(\eta^6\text{-}p\text{-cymene})(L)(Cl)] + H_2O \quad (2)^a$$

[a] Charges are omitted.

Based on these equilibrium constants, concentration distribution curves were calculated for the complexes [ML] at various chloride concentrations (Fig. 7).

Fig. 6

Fig. 7

The complex of dipic has a log*K** value about an order of magnitude lower than pic, thus, resulting in less favourable formation of the chlorido complex [Ru(II)(η^6-*p*-cymene)(L)Cl]. The coordination of the negatively-charged chloride ions to neutral [Ru(II)(η^6-*p*-cymene)(dipic)(H_2O)] with a non-coordinated carboxylate moiety seems to be less pronounced than to the positively charged aqua complex of pic and 6-Mepic. This finding may contribute to the explanation of the lower biological activity of the dipic complex compared with that of pic [36,48], in terms of showing higher reactivity to blood serum components. Such binding takes place by replacing the coordinated water molecule, while the neutral complex [Ru(II)(η^6-*p*-cymene)(L)Cl] of pic remains intact to a higher degree facilitating crossing cell membranes.

The pyridine-N is able to coordinate monodentately to the Ru center in absence of a second donor atom to act as a chelating ligand [36]. In order to exclude the possibility of the formation of bis-ligand Ru(II)(η^6-*p*-cymene) complexes of the pyridinecarboxylates in which one of the ligands binds via the (N,O) donor set and the other monodentately, pH-dependent ^{1}H NMR spectra were recorded at 1:2 metal-to-ligand ratio (not shown). Indeed, only species already identified in the measurements at 1:1 metal-to-ligand ratio were found. Additionally, spectra were collected at various metal-to-ligand ratios at a pH value at which [ML] predominates (see Fig. S6 for pic). Peaks being assigned merely to the species in the equilibria (2) and (3) were found. Hence, there is no indication for bis-ligand complex formation.

$$M + HL \rightleftharpoons [ML] + H^+ \qquad (3)$$

In order to compare the differences in speciation and thus in the stability of the complexes formed in the [Ru(II)(η^6-*p*-cymene)]−pyridinecarboxylate systems, concentration distribution curves were calculated under the same conditions with the help of the logβ values determined for the species [MLH], [ML] and [MLH_{-1}] by pH-potentiometry and UV/Vis spectrophotometry (Table 1, Fig. 8). The predominant formation of the species [ML] is found in all cases at physiological pH. The ratio of the non-bound metal ion in the acidic pH range follows the order of dipic < pic < 6-Mepic reflecting the stability trend of the complexes formed, namely dipic > pic > 6-Mepic. Taking the different basicities of these ligands into consideration, the logβ [ML] values were corrected according to the competition equilibrium (3) and log*K'* (= logβ [ML] – pK_a (HL)) derived constants were calculated (Table 1). A higher log*K*' implies more favoured metal complex formation as compared with the protonated

ligand (HL). These values also indicate that the presence of methyl or an additional carboxylic acid functionality at the pyridine ring of pic has a distinct influence on the speciation. 6-Mepic forms lower stability complexes, while the coordination compounds of dipic are somewhat more stable than that of pic. This trend was also shown for *e.g.* Zn(II) and V(IV)O complexes [45,54]. The more compact size of pic compared with that of 6-Mepic may result in higher stability; while the coordination of the dipic ligand in its L^{2-} form seems to be advantageous over the binding of monovalent picolinate to the positively charged organometallic centre.

Comparing the stabilities of Ru(II)(η^6-*p*-cymene) complexes formed with the picolinates to those of bidentate (O,O) hydroxypyr(id)ones [24,53,55] or (O,S) hydroxythiopyr(id)ones [37] taking into consideration the different basicities of the ligands the following stability trend is seen: (O,S) > (O,N) > (O,O), which corresponds well to their order of biological activity [28,30,36,47-49].

Fig. 8

4. Conclusions

The speciation of ruthenium(II)-η^6-*p*-cymene complexes of the pyridinecarboxylic acid pic and its derivatives dipic and 6-Mepic containing methyl or carboxylate functionalities at position (6) was characterized in aqueous solution via a combined approach using pH-potentiometry, ^{1}H NMR spectroscopy and UV/Vis spectrophotometry. These ligands form exclusively mono-ligand [ML] (and [MLH] in the case of dipic) complexes with high stabilities in which the ligands coordinate in a bidentate (O,N) fashion. Hydrolysis of these complexes results in the formation of the mixed-hydroxido species [ML(OH)] only in the basic pH range, although this process is almost negligible at physiological pH. No decomposition of the Ru(II)(η^6-*p*-cymene)−pic complexes was found at pH < 11 even after 24 h, while formation of the dinuclear trihydroxido-bridged species $[Ru_2(\eta^6\text{-}p\text{-cymene})_2(OH)_3]^+$ and the liberation of the non-bound ligand in a slow reaction was detected already at pH ~10 in the case of complexes of 6-Mepic and dipic. The Ru(II)(η^6-*p*-cymene) binding ability of the ligands shows the following order: 6-Mepic < pic < dipic. The increased stability of the complexes of picolinates compared to that of the (O,O) donor hydroxypyrones may be related to their higher biological activity.

The aquation of the [Ru(II)(η^6-*p*-cymene)(L)Cl] has a strong impact on the bioactivity and, therefore, the Cl^-/H_2O co-ligand exchange process was also studied by ^1H NMR spectroscopy and quite similar equilibrium constants were found for the complexes of pic and its 6-methyl derivative, while complex [ML] of dipic has much weaker ability to retain the chloride at the third coordination site.

Acknowledgments

This work was supported by the Hungarian Research Foundation OTKA 103905 project and É.A. Enyedy gratefully acknowledges the financial support of J. Bolyai research fellowship. This research was realized in the frames of TÁMOP 4.2.4. A/2-11-1-2012-0001 „National Excellence Program – Elaborating and operating an inland student and researcher personal support system" The project was subsidized by the European Union and co-financed by the European Social Fund.. We thank Ms. Bella Bruszel for conducting some of the experiments.

Appendix A. Supplementary data

Table containing the chemical shifts of the HL and L ligand species, UV/Vis absorbance spectra of the [Ru(II)(η^6-*p*-cymene)]−pic system, ^1H NMR spectra of [Ru(II)(η^6-*p*-cymene)$(H_2O)_3]^{2+}$−pic system (time dependence, at various metal-to-ligand ratios), [Ru(II)(η^6-*p*-cymene)]−6-Mepic system at pH 10.6, Ru(II)(η^6-*p*-cymene)$(H_2O)_3]^{2+}$−dipic system at various chloride concentrations.

References

[1] A.K. Fink, R.R. German, M. Heron, S.L. Stewart, C.J. Johnson, J.L. Finch, D. Yin, P.E. Schaeffer, Cancer Epidemiology 36 (2012) 22.

[2] C.J. Johnson, H.K. Weir, A.K. Fink, R.R. German, J.L. Finch, R.K. Rycroft, D. Yin, Cancer Epidemiology 37 (2013) 20.

[3] M. Rosenberg, L. VanCamp, T. Krigas, Nature 205 (1965) 698.

[4] E. Wong, C.M. Giandomenico, Chem. Rev. 99 (1999) 2451.

[5] F. Muggia, Gynecologic Oncology 112 (2009) 275.

[6] N. Kröger, U.R. Kleeberg, K. Mross, L. Edler, D.K. Hossfeld, Onkologie 23 (2000) 60.

[7] M.A. Jakupec, B.K. Keppler, Curr. Top. Med. Chem. 4 (2004) 1575.

[8] E. Alessio, G. Mestroni, A. Bergamo, G. Sava, Curr. Top. Med. Chem. 4 (2004) 1525.

[9] C.G. Hartinger, M.A. Jakupec, S. Zorbas-Seifried, M. Groessl, A. Egger, W. Berger, H. Zorbas, P.J. Dyson, B.K. Keppler, Chem. Biodiversity 5 (2008) 2140.

[10] C.G. Hartinger, S. Zorbas-Seifried, M.A. Jakupec, B. Kynast, H. Zorbas, B.K. Keppler, J. Inorg. Chem. 100 (2006) 891.

[11] P. Heffeter, K. Böck, B. Atil, M.A.R. Hoda, W. Körner, C. Bartel, U. Jungwirth, B.K. Keppler, M. Micksche, W. Berger, G. Koellensperger, J. Biol. Inorg. Chem. 15 (2010) 737.

[12] G. Sava, E. Alessio, A. Bergamo, G. Mestroni, Top. Biol. Inorg. Chem. 1 (1999) 143.

[13] G. Sava, I. Capozzi, K. Clerici, G. Gagliardi, E. Alessio, G. Mestroni, Clin. Exp. Metastasis 16 (1998) 371.

[14] A. Levina, A. Mitra, P.A. Lay, Metallomics 1 (2009) 458.

[15] L. Trynda-Lemiesz, A. Karaczyn, B.K. Keppler, H. Kozlowski, J. Inorg. Biochem. 78 (2000) 341.

[16] L. Trynda-Lemiesz, B.K. Keppler, H. Kozlowski, J. Inorg. Biochem. 73 (1999) 123.

[17] O. Mazuryk, K. Kurpiewska, K. Lewiński, G. Stochel, M. Brindell, J. Inorg. Biochem. 116 (2012) 11.

[18] A. Calzolari, I. Oliviero, S. Deaglio, G. Mariani, M. Biffoni, N.M. Sposi, F. Malavasi, C. Peschle, U. Testa, Blood Cells Mol. Dis. 39 (2007) 82.

[19] S. Kapitza, M.A. Jakupec, M. Uhl, B.K. Keppler, B. Marian, Cancer Lett. 226 (2005) 115.

[20] K.S. Smalley, R. Contractor, N.K. Haass, A.N. Kulp, G.E. Atilla-Gokcumen, D.S. Williams, Cancer Res. 67 (2007) 209.

[21] W.H. Ang, A. Casini, G. Sava, P.J. Dyson, J. Org. Chem. 696 (2011) 989.

[22] B. Therrien, Coord. Chem. Rev. 253 (2009) 493.

[23] O. Nováková, A.A. Nazarov, C.G. Hartinger, B.K. Keppler, V. Brabec, Biochem. Pharm. 77 (2009) 364.

[24] P. Buglyó, E. Farkas, Dalton Trans. 39 (2009) 8063.

[25] L. Bíró, E. Farkas, P. Buglyó, Dalton Trans. 41 (2012) 285.

[26] N. Gligorijević, S. Aranđelović, L. Filipović, K. Jakovljević, R. Janković, S. Grgurić-Šipka, I. Ivanović, S. Radulović, Ž. Lj. Tešić, J. Inorg. Biochem. 108 (2012) 53.

[27] C.A. Vock, A.K. Renfrew, R. Scopelliti, L. Juillerat-Jeanneret, P.J. Dyson, Eur. J. Inorg. Chem. (2008) 1661.

[28] W. Kandioller, C.G. Hartinger, A.A. Nazarov, M.L. Kuznetsov, R.O. John, C. Bartel, M.A. Jakupec, V.B. Arion, B.K. Keppler, Organometallics 28 (2009) 4249.

[29] W. Kandioller, A. Kurzwernhart, M. Hanif, S.M. Meier, H. Henke, B.K. Keppler, C.G. Hartinger, J. Organomet. Chem. 696 (2011) 999.

[30] W. Kandioller, C.G. Hartinger, A.A. Nazarov, C. Bartel, M. Skocic, M.A. Jakupec, V.B. Arion, B.K. Keppler, Chem. Eur. J. 15 (2009) 12283.

[31] J. Kljun, A.K. Bytzek, W. Kandioller, C. Bartel, M.A. Jakupec, C.G. Hartinger, B.K. Keppler, I. Turel, Organometallics 30 (2011) 2506.

[32] W.H. Ang, A. Casini, G. Sava, P.J. Dyson, J. Organomet. Chem. 696 (2011) 989.

[33] A.M. Pizarro, M. Melchart, A. Habtemariam, L. Salassa, F.P.A. Fabbiani, S. Parsons, P.J. Sadler, Inorg. Chem. 49 (2010) 3310.

[34] F. Wang, H. Chen, S. Parsons, I.D.H. Oswald, J.E. Davidson, P.J. Sadler, Chem. Eur. J. 9 (2003) 5810.

[35] F. Beckford, J. Thessing, J. Woods, J. Didion, N. Gerasimchuk, A. Gonzalez-Sarrias, N.P. Seeram, Metallomics 3 (2011) 491.

[36] S. Grgurić-Šipka, I. Ivanović, G. Rakić, N. Todorović, N. Gligorijević, S. Radulović, V.B. Arion, B.K. Keppler, Ž.Lj. Tešić, Eur. J. Med. Chem. 45 (2010) 1051.

[37] E.A. Enyedy, E. Sija, T. Jakusch, C.G. Hartinger, W. Kandioller, B.K. Keppler, T. Kiss, J. Inorg. Chem. doi: 10.1016/j.jinorgbio.2013.05.002

[38] P. Gans, A. Sabatini, A. Vacca, Talanta 43 (1996) 1739.

[39] M.A. Bennett, T.N. Huang, T.W. Matheson, A.K. Smith, Inorg. Synth. 21 (1982) 74.

[40] H.M. Irving, M.G. Miles, L.D. Pettit, Anal. Chim. Acta 38 (1967) 475.

[41] SCQuery, The IUPAC Stability Constants Database, Academic Software (version 5.5), Royal Society of Chemistry, 1993–2005.

[42] L. Zékány, I. Nagypál, Computational Methods for the Determination of Stability Constants (Ed.: D. L. Leggett), Plenum Press, New York, 1985, 291–353.

[43] E. Kiss, E. Garribba, G. Micera, T. Kiss, H. Sakurai, J. Inorg. Biochem. 78 (2000) 97.

[44] T. Jakusch, W. Jin, L. Yang, T. Kiss, D.C. Crans, J. Inorg. Biochem. 95 (2003) 1.

[45] É.A. Enyedy, A. Lakatos, L. Horváth, T. Kiss, J. Inorg. Biochem. 102 (2008) 1473.

[46] R. Lang, K. Polborn, T. Severin, K. Severin, Inorg. Chim. Acta 294 (1999) 62.

[47] W. Kandioller, C.G. Hartinger, A.A. Nazarov, J. Kasser, R. John, M.A. Jakupec, V.B. Arion, P.J. Dyson, B.K. Keppler, J. Organomet. Chem. 694 (2009) 922.

[48] I. Ivanović, S. Grgurić-Šipka, N. Gligorijević, S. Radulović, A. Roller, Ž.L. Tešić, B.K. Keppler, J. Serb. Chem. Soc. 76 (2011) 53.

[49] M. Hanif, H. Henke, S.M. Meier, S. Martic, M. Labib, W. Kandioller, M.A. Jakupec, V.B. Arion, H.B. Kraatz, B.K. Keppler, C.G. Hartinger, Inorg. Chem. 49 (2010) 7953.

[50] Z. Vargová, V. Zeleňák, I. Císařová, K. Györyová, Thermochim. Acta 423 (2004) 149.

[51] O.Z. Yeşilel, İ. İlker, M.S. Refat, H. Ishida, Polyhedron 29 (2010) 2345.

[52] T.S. Kamatchi, N. Chitrapriya, H. Lee, C.F. Fronczek, F.R. Fronczek, K. Natarajan, Dalton Trans. 41 (2012) 2066.

[53] E.A. Enyedy, G.M. Bognar, T. Kiss, M. Hanif, C.G. Hartinger, J. Organomet. Chem. 734 (2013) 38.

[54] T. Jakusch, K. Gajda-Schrantz, Y. Adachi, H. Sakurai, T. Kiss, L. Horváth, J. Inorg. Biochem. 100 (2006) 1521.

[55] L. Bíró, E. Farkas, P. Buglyó, Dalton Trans. 39 (2010) 10272.

Table 1

Proton dissociation constants (pK_a) of pic, 6-Mepic and dipic; overall (logβ ($M_pL_qH_r$)), stepwise and derived stability constants of their Ru(II)-(η^6-*p*-cymene) complexes [T = 25.0 °C; I = 0.20 M (KCl)][a]

		pic[b]	pic	6-Mepic	dipic
pH-metry	**pK_a (H_3L)** (COOH)	–	–	–	< 1
	pK_a (H_2L) (COOH)	~ 1	~ 1	~ 1	2.01(3)
	pK_a (HL) ($N_{pyridine}$)	5.15(1)	5.17(1)	5.82(1)	4.59(1)
UV/Vis	**log β (MLH)**	–	–	–	12.4(3)
	log β (MLH_{-1})	8.90(1)	8.14(1)	7.44(1)	11.25(9)
	pK (MLH) = log β (MLH) − log β (ML)	0.90(2)	-0.76(2)	-1.63(4)	2.40(5)
	pK (ML) = log β (ML) − log β (MLH_{-1})	–	–	–	1.15
	log$K$' (ML) = log β (ML) − pK_a (HL)	8.00	8.90	9.07	8.90
pH-metry	**log β (MLH_{-1})**	3.75	2.97	1.62	4.65[c]
	pK (ML) = log β (ML) - log β (MLH_{-1})	0.86(2)	-0.75(2)	-1.60(3)	2.27(5)
^{1}H NMR	**pK (ML)**	8.04	8.90	9.04	8.98
	log$K$* (H_2O/Cl^-)[d]	8.10	–	–	–
		–	1.83(6)	1.45(5)	0.7(1)

[a] Uncertainties (SD) are shown in parentheses for the species characterized in the present work. Charges are omitted for simplicity. M denotes [Ru(η^6-*p*-cymene)]. Hydrolysis products of the organometallic fragment: logβ $[Ru_2(\eta^6\text{-}p\text{-cymene})_2H_{-2}]^{2+}$ = −6.97(2) obtained by pH-metry, −7.02(5) by UV/Vis and logβ $[(Ru_2(\eta^6\text{-}p\text{-cymene})_2H_{-3}]^+$ = −11.97(1) by pH-metry, −11.68(6) by UV/Vis.

[b] Determined at I = 0.20 M (KNO_3). Hydrolysis products: logβ $[(Ru_2(\eta^6\text{-}p\text{-cymene})_2H_{-3}]^+$ = −9.36(2) obtained by pH-metry and −9.33(2) by UV/Vis.

[c] log β (ML) – pK_a (HL) – pK_a (H_2L)

[d] $[Ru(\eta^6\text{-}p\text{-cymene})(L)(H_2O)]^+ + Cl^- \rightleftharpoons [Ru(\eta^6\text{-}p\text{-cymene})(L)(Cl)] + H_2O$ determined at various total concentrations of chloride ions.

Legends to Figures

Chart 1. Chemical formulae of the ligands in their neutral forms

Fig. 1. Low-field regions of the ^{1}H NMR spectra recorded for the [Ru(η^6-*p*-cymene)$(H_2O)_3]^{2+}$−pic system at the indicated pH values. *Symbols: CH*(6) of ligand: ● in $[Ru(\eta^6\text{-}p\text{-cymene})(L)(H_2O)]^+$; *CH*(5) of ligand: ■ in $[Ru(\eta^6\text{-}p\text{-cymene})(L)(H_2O)]^+$; *CH*(3) of ligand: ▲ in $[Ru(\eta^6\text{-}p\text{-cymene})(L)(H_2O)]^+$; *CH*(4) of ligand: ★ in $[Ru(\eta^6\text{-}p\text{-cymene})(L)(H_2O)]^+$; *Ar*(*CH*) of *p*-cymene moiety: ♦ in $[Ru(\eta^6\text{-}p\text{-cymene})(L)(H_2O)]^+$; [$c_L = c_M = 1.0 \times 10^{-3}$ M; T = 25.0 °C; I = 0.20 M (KNO_3); 10% (v/v) D_2O].

Fig. 2. pH-Potentiometric titration curves for dipic (●) and for the [Ru(II)(η^6-*p*-cymene)]−dipic system at different metal-to-ligand ratios. M:L ratios: (×) 1:1; (◊) 1:2; (-) 1:4. [$c_L = 2.0 \times 10^{-3}$ M, T = 25.0 °C, I = 0.2 M (KCl)]

Fig. 3. UV/Vis absorbance spectra of the [Ru(II)(η^6-*p*-cymene)]−dipic system recorded in the pH range of 1 − 2 (solid lines) on individual samples. *The inset shows the spectra of the ligand (dotted line) and the metal ion alone (dashed line) for comparison at pH 2 at the same concentrations.* [$c_L = c_M = 1.2 \times 10^{-4}$ M, T = 25.0 °C, I = 0.2 M (KCl/HCl)]

Fig. 4. Low-field regions of the ^{1}H NMR spectra recorded for the [Ru(II)(η^6-*p*-cymene)$(Z)_3$]−dipic system at the indicated pH values [$c_L = c_M = 2.0 \times 10^{-3}$ M, T = 25.0 °C, I = 0.2 M (KCl), 10% (v/v) D_2O]. *The inset shows the pH-dependence of the ^{1}H NMR chemical shifts of the CH(4) peaks of the ligand in the mono-ligand complexes. Symbols: CH*(4) of ligand: ● in $[ML(H_2O)]$, ○ in $[MLCl]^-$; *Ar(CH)* of *p*-cymene: ♦ in [MLZ] (Z = H_2O or Cl^-).

Fig. 5. Low-field regions of the ^{1}H NMR spectra recorded for the [Ru(II)(η^6-*p*-cymene)]−pic system at the indicated pH values. The framed details of spectra with dashed line indicate where would be the *Ar(CH)* signals of $[M_2H_{-3}]^+$ in case of decomposition. *Symbols: CH*(6) of ligand: ● in $[ML(H_2O)]^+$, ○ in [MLCl], ● in $[MLH_{-1}]$; *CH*(5) of ligand: ■ in $[ML(H_2O)]^+$, □ in [MLCl], ■ in $[MLH_{-1}]$; *CH*(3) of ligand: ▲ in $[ML(H_2O)]^+$, Δ in [MLCl], ▲ in $[MLH_{-1}]$; *CH*(4) of ligand: ★ in $[ML(H_2O)]^+$, ✯ in [MLCl], ★ in $[MLH_{-1}]$; *Ar*(*CH*) of *p*-cymene: ♦ in $[ML(H_2O)]^+$, ◊ in [MLCl], ♦ in $[MLH_{-1}]$. [$c_L = c_M = 1.0 \times 10^{-3}$ M, T = 25.0 °C, I = 0.2 M (KCl), 10% (v/v) D_2O]

Fig. 6. Low-field regions of the ^{1}H NMR spectra recorded for the [Ru(II)(η^6-*p*-cymene)$(H_2O)_3]^{2+}$−pic system at various chloride concentrations at pH 3.2. *Symbols: CH*(6) of ligand: ● in $[ML(H_2O)]^+$, ○ in [MLCl]; *CH*(5) of ligand: ■ in $[ML(H_2O)]^+$, □ in [MLCl]; *CH*(3) of ligand: ▲ in $[ML(H_2O)]^+$, Δ in [MLCl]; *CH*(4) of ligand: ★ in $[ML(H_2O)]^+$, ☆ in [MLCl]; *Ar(CH)* of *p*-cymene: ♦ in $[ML(H_2O)]^+$, ◊ in [MLCl]. [$c_L = c_M = 2.0 \times 10^{-3}$ M; T = 25.0 °C, 10% D_2O]

Fig. 7. Concentration of distribution curves of the [Ru(II)(η^6-*p*-cymene)]−(N,O) ligand systems on the basis of log$K$* values (pic (continuous lines), 6-Mepic (dashed lines), dipic (dotted lines)). [pH = 3.2 (pic, dipic); 4.0 (6-Mepic); $c_{[ML]} = 1.0 \times 10^{-3}$ M; T = 25.0 °C]

Fig. 8. Concentration distribution curves for [Ru(II)(η^6-*p*-cymene)]−pic (continuous black lines); [Ru(II)(η^6-*p*-cymene)]−6-Mepic (dashed black lines) and [Ru(II)(η^6-*p*-cymene)]−dipic (dotted grey lines) systems. [$c_L = c_M = 2.0 \times 10^{-3}$ M, T = 25.0 °C, I = 0.2 M (KCl)]

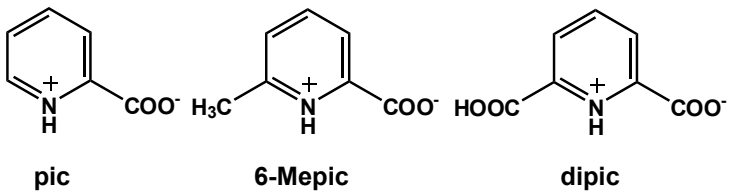

Chart 1.

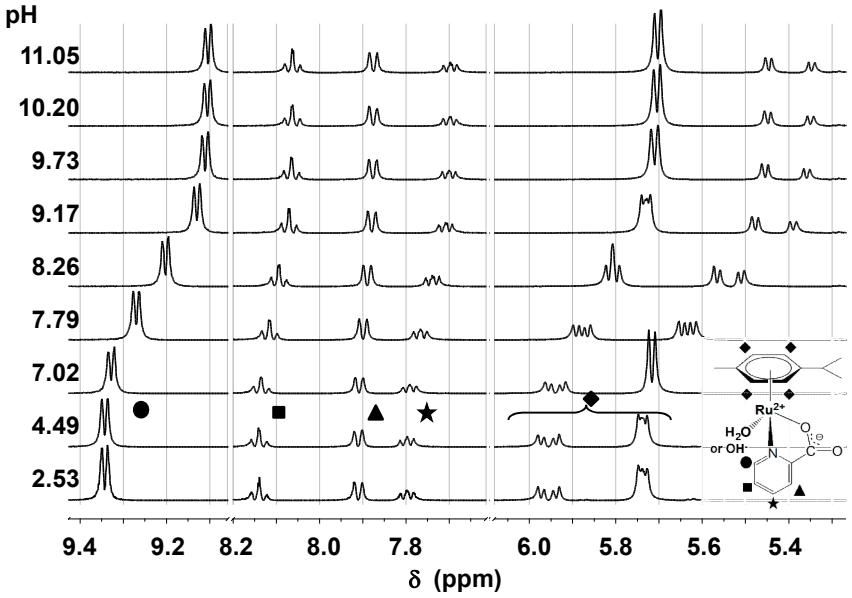

Fig. 1.

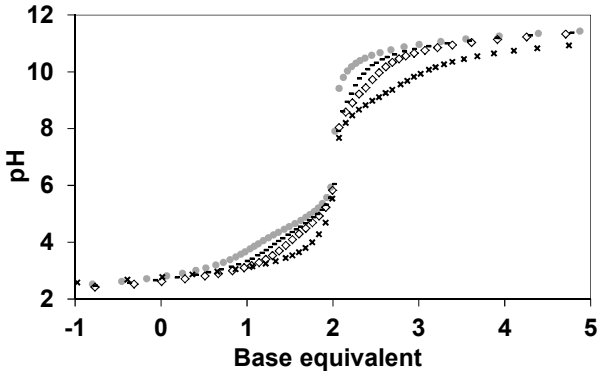

Fig. 2.

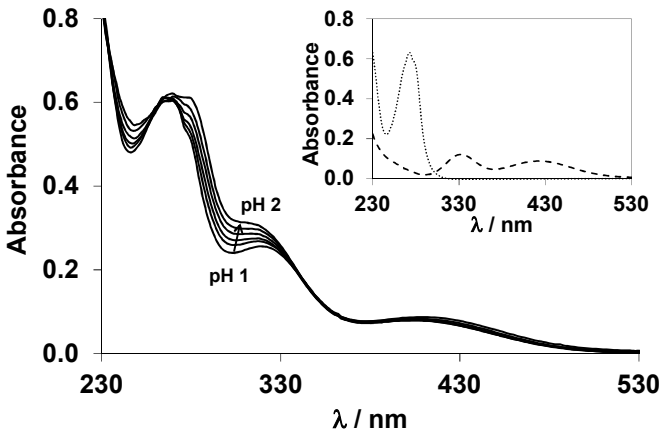
Absorbance
0.8
0.6
0.4
0.2
0.0
230
330
430
530
λ / nm
pH 2
pH 1
Absorbance
0.8
0.6
0.4
0.2
0.0
230
330
430
530
λ / nm

Fig. 3.

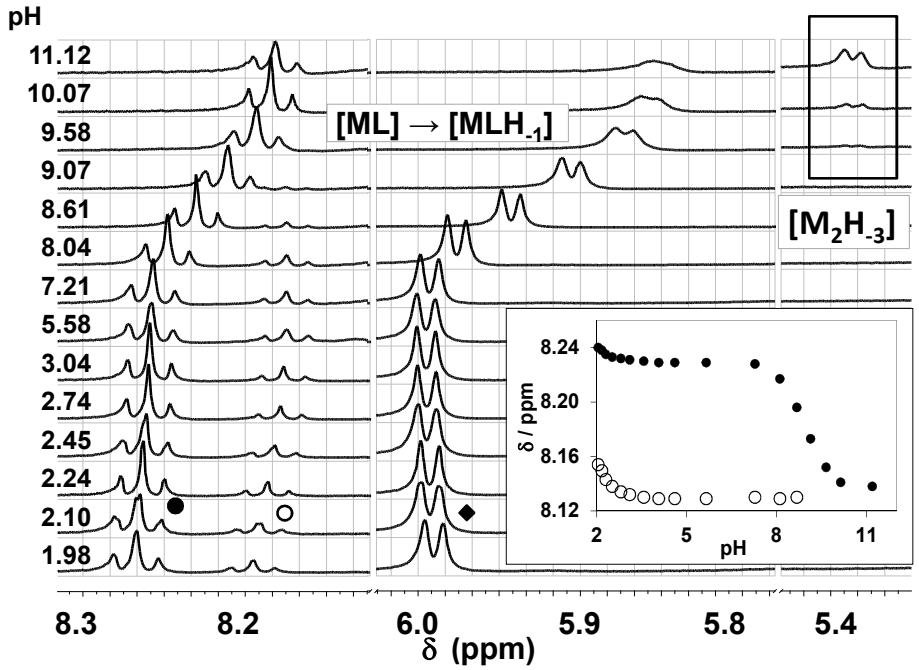
pH
11.12
10.07
9.58
9.07
8.61
8.04
7.21
5.58
3.04
2.74
2.45
2.24
2.10
1.98
[ML] → [MLH-1]
[M2H-3]
8.24
8.20
8.16
8.12
δ / ppm
2
5
8
11
pH
8.3
8.2
6.0
5.9
5.8
5.4
δ (ppm)

Fig. 4.

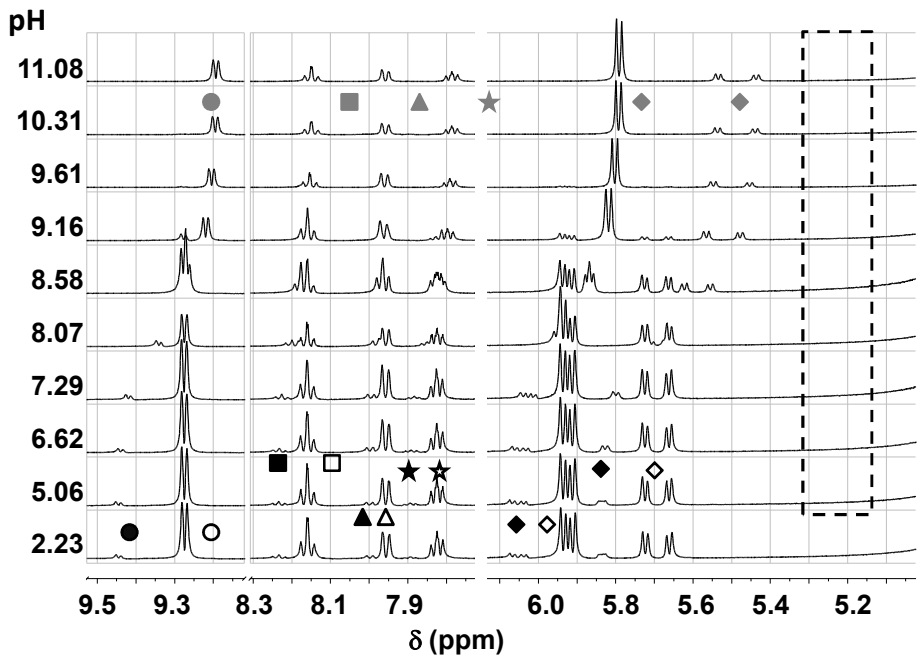
pH
11.08
10.31
9.61
9.16
8.58
8.07
7.29
6.62
5.06
2.23
9.5
9.3
8.3
8.1
7.9
6.0
5.8
5.6
5.4
5.2
δ (ppm)

Fig. 5.

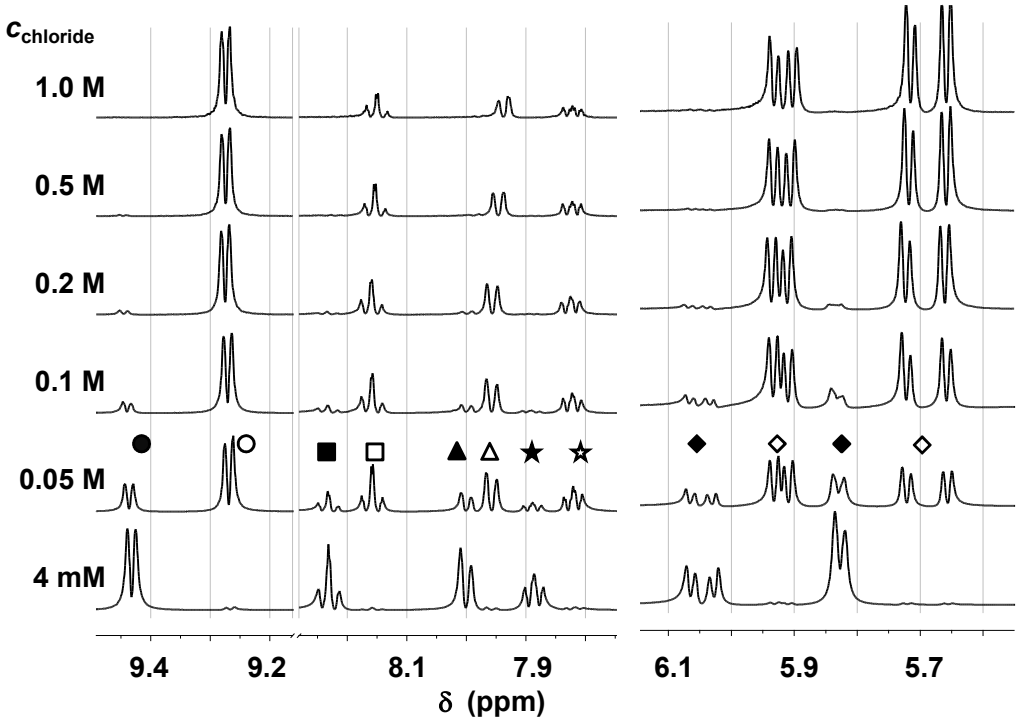
$c_{chloride}$
1.0 M
0.5 M
0.2 M
0.1 M
0.05 M
4 mM
9.4
9.2
8.1
7.9
6.1
5.9
5.7
δ (ppm)

Fig. 6.

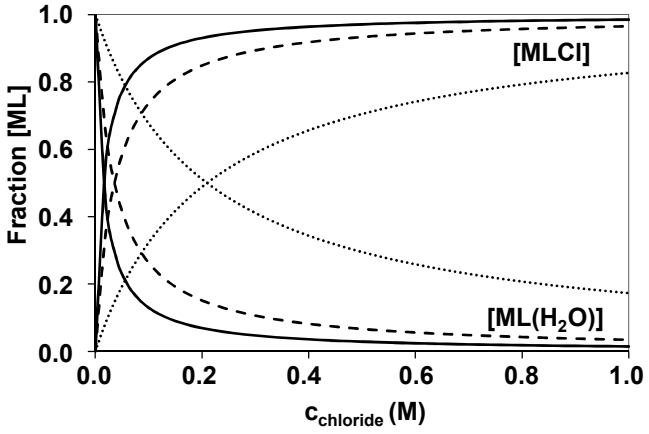
Fraction [ML]
1.0
0.8
0.6
0.4
0.2
0.0
0.0
0.2
0.4
0.6
0.8
1.0
[MLCl]
[ML(H2O)]
cchloride (M)

Fig. 7.

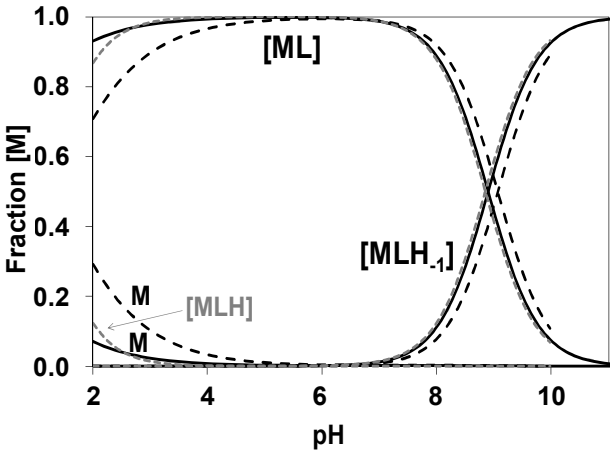

Fig. 8.